Article (refereed) - postprint

Contact CEH NORA team at
noraceh@ceh.ac.uk

Methanotrophic activity in slurry surface crusts as influenced by CH$_4$, O$_2$, and inorganic N

Yun-Feng Duan [1] *, Sabine Reinsch [2] #, Per Ambus [2] §, Lars Elsgaard [1], and Søren O. Petersen [1]

[1] Department of Agroecology, Aarhus University, Blichers Allé 20, DK-8830 Tjele, Denmark

[2] Department of Chemical and Biochemical Engineering, Technical University of Denmark, Frederiksborgvej 399, DK-4000 Roskilde, Denmark

* Corresponding Author: Yun-Feng Duan, Department of Agroecology, Aarhus University, Blichers Allé 20, DK-8830 Tjele, Denmark; E-mail: Kevin.YF.Duan@gmail.com.

Present address: Centre for Ecology and Hydrology, Deiniol Rd, Bangor Gwynedd, LL57 2 UW, UK

§ Present address: Department of Geosciences and Natural Resource Management, University of Copenhagen, Øster Voldgade 10, DK-1350 Copenhagen, Denmark

Abbreviations

MOB: Methane oxidizing bacteria; PLFA: Phospholipid fatty acid; FAME: Fatty acid methyl esters

Keywords

Methane oxidation; Inorganic nitrogen; Microsensor; PLFA stable-isotope probing; Methane oxidizing bacteria.

Core Ideas

- Oxygen penetration into surface crusts is shallow.
- Nitrous oxide accumulates at oxic-anoxic interfaces in surface crusts.
- Oxygen availability is important to high-concentration methane oxidation.
- Microbial methane oxidation is affected by interactions of inorganic N and oxygen.
- Activity of Type I methanotrophs dominates under high methane concentration.

Abstract

Livestock slurry is a major source of atmospheric CH_4, but surface crusts harboring methane oxidizing bacteria (MOB) could mediate against CH_4 emissions. This study examined conditions for methane oxidation by *in-situ* measurements of O_2 and N_2O, as a proxy for inorganic N transformations, in intact crusts using microsensors. This was combined with laboratory incubations of crust material to investigate effects of O_2, CH_4, and inorganic N on methane oxidation, using $^{13}CH_4$ to trace C incorporation into lipids of MOB. Oxygen penetration into the crust was 2–14 mm, confining the potential for aerobic methane oxidation to a shallow layer. Nitrous oxide accumulated within or below the zone of O_2 depletion. With 10^2 ppmv CH_4 there was no O_2 limitation on methane oxidation at O_2 concentrations as low as 2%, whereas methane oxidation at 10^4 ppmv CH_4 was reduced at $\leq 5\%$ O_2. As hypothesized, methane oxidation was in general inhibited by inorganic N, especially NO_2^-, and there was an interaction between N inhibition and O_2 limitation at 10^2 ppmv CH_4, as indicated by consistently stronger inhibition of methane oxidation by NH_4^+ and NO_3^- at 3% compared to 20% O_2. Recovery of ^{13}C in phospholipid fatty acids suggested that both Type I and Type II MOB were active, with Type I dominating high-concentration methane oxidation. Given the structural heterogeneity of crusts, methane oxidation activity likely varies spatially as constrained by the combined effects of CH_4, O_2, and inorganic N availability in microsites.

Introduction

In regions with intensive livestock production such as Western Europe and North America, up to 40% of livestock CH_4 emissions may be related to manure management (Francesco et al., 2013). In most cases, CH_4 capture and/or biofiltration is neither technically feasible nor economical (Melse and van der Werf, 2005), and more cost-effective alternatives must be considered. When manure is stored as liquid slurry, a dense floating crust is often formed either naturally from dry matter in the slurry, or by facilitation of admixing with chopped straw (Hansen et al., 2009). Studies have demonstrated a potential for aerobic methane oxidation in such surface crusts (Petersen and Ambus, 2006; Petersen et al., 2005), where diverse communities of methane-oxidizing bacteria (MOB) were also documented (Duan et al., 2014). These findings

26   suggest that surface crusts could act as a low-cost filter for manure-derived CH_4, but the physical, chemical,

27   and biological regulation of methane oxidation inside crusts is largely unknown.

28   Methane oxidation potential depends on CH_4 and O_2 availability, which are highly variable due to the

29   heterogeneous structure of the crust. Since surface crusts overlie liquid manure with a high methanogenic

30   potential, they are typically high-CH_4 environments with concentrations far above the atmospheric level. We

31   have observed up to 200 ppmv CH_4 in the stagnant atmosphere immediately above the surface crust (Y.F.

32   Duan, unpublished data), and headspace CH_4 concentrations of 10^2 and 10^4 ppmv were used previously to

33   simulate this range of CH_4 availability for MOB in laboratory incubations (Duan et al., 2013). Due to the often

34   loose structure of the crust, sectioning for extraction and determination of *in situ* CH_4 availability by

35   sampling are impractical. While a CH_4 biosensor has been described (Damgaard and Revsbech, 1997), it is

36   not commercially available and has not been tested in heterogeneous environments such as surface crusts.

37   In contrast to CH_4, the distribution of O_2 in surface crusts can be readily determined using a microsensor

38   (Revsbech, 2005), as demonstrated by Hansen et al. (2009) and Nielsen et al. (2010) who investigated O_2

39   penetration into various slurry crusts.

40   Inhibition of methane oxidation by inorganic N is known from many environments (Bosse et al., 1993;

41   Dunfield and Knowles, 1995; Wang and Ineson, 2003), as well as in surface crusts (Duan et al., 2013), but

42   stimulation or no effect can also occur (Liu and Greaver, 2009). Livestock slurry and surface crusts are highly

43   enriched in inorganic N (Table 1): the slurry phase may contain up to 200 mM ammoniacal N (NH_3/NH_4^+)

44   (Nielsen et al., 2010; Sommer et al., 2007), while up to 35 mM NO_3^- (Hansen et al., 2009) and 98 mM NO_2^-

45   (Nielsen et al., 2010) have been found at the oxic-anoxic interface in surface crusts. These concentration

46   ranges (Table 1) represent a high variability of inorganic N at microsites within surface crusts due to

47   fluctuations in water content as a result of precipitation and insolation (Nielsen et al., 2010). Due to this

48   heterogeneity, bulk N concentrations are insufficient to characterize N distribution and thus potential

49   interference with methane oxidation in microsites. While specialized sensors are available to determine

50   micro-scale concentrations of NH_4^+, NO_2^-, and NO_3^- in aqueous environments (De Beer et al., 1997; De Beer

et al., 1991; Larsen et al., 1996), they are difficult to apply in unsaturated matrices such as surface crusts, where contact to liquid phase may be intermittent. Instead, the accumulation of N_2O in the crust was used in this study as a proxy for the distribution of N transformations and thus presence of inorganic N (Larsen et al., 1996), as both nitrification and denitrification can produce N_2O under sub-oxic conditions (Bollmann and Conrad, 1998).

The effects of environmental factors on methane oxidation in surface crusts will ultimately depend on the MOB present (Bodelier, 2011; Hu and Lu, 2015). Aerobic MOB have been conventionally categorized into Type I and Type II based on phylogenetic and functional traits, including the presence of signature 16-carbon (C_{16}) or 18-carbon (C_{18}) phospholipid fatty acids (PLFAs) (Hanson and Hanson, 1996). Type I MOB have been reported to thrive in N-sufficient, high-O_2 and low-CH_4 environments, whereas Type II MOB seem to favor the opposite (Amaral et al., 1995; Amaral and Knowles, 1995; Graham et al., 1993). It is still unclear to what extent CH_4, O_2, and inorganic N conditions will select one type of MOB over another in surface crusts, but previous studies found that Type I MOB are more abundant and diverse than Type II MOB in this environment (Duan et al., 2014; Hansen et al., 2009; Nielsen et al., 2013). In recent years, novel methane oxidation pathways, such as NO_2^- dependent anaerobic methane oxidation (Ettwig et al., 2010; Welte et al., 2016), as well as aerobic methane oxidation coupled with partial denitrification (Kits et al., 2015a; Kits et al., 2015b), have also been described, but the importance of these processes and the presence of relevant microorganisms in surface crusts remain unclear.

A main objective of this study was to examine the potential for microbial methane oxidation under realistic storage conditions by characterizing *in situ* distributions of O_2 and inorganic N transformations in a cattle slurry surface crust using microsensors. Effects and interactions of O_2 and inorganic N species with respect to methane oxidation could not be quantified *in situ* where microbial activities occur in micro-sites, and instead this was investigated under controlled laboratory conditions. Here, $^{13}CH_4$ was used as substrate, allowing ^{13}C stable isotope probing of PLFAs to study the involvement of Type I and Type II MOB in methane oxidation in surface crusts. Based on previous results (Duan et al., 2014; Duan et al., 2013) we hypothesized that

76   methane oxidation activity in surface crusts would be determined by both CH_4 and O_2 availability, and

77   inhibited by inorganic N, and that Type I MOB would be primarily responsible for methane oxidation.

Materials and Methods

Microsensor Measurement of O_2 and N_2O Distribution

80   Dairy cattle slurry was collected from a full-scale manure storage facility in May, 2012, and transferred to

81   two tanks at a pilot-scale storage system (Petersen et al., 2009) at Aarhus University (Foulum, Denmark). The

82   slurry was stored for six weeks prior to the measurement in June, by which time a 5–6 cm thick surface crust

83   with a stable structure had developed on top of the slurry. The development of surface crust reflected

84   typical storage conditions, where a new crust is formed following the mixing of slurry in spring for field

85   application.

86   Oxygen and N_2O concentration profiles in the surface crust were determined using, respectively, an O_2 and a

87   N_2O microsensor with a tip diameter of 0.5 mm (both produced by Unisense, Aarhus, Denmark). Both

88   microsensors were calibrated according to manufacturer's instructions. Detection limits for O_2 and N_2O were

89   0.3 µmol L^{-1} and 0.1 µmol L^{-1}, respectively.

90   A custom-made mounting system was used to place the microsensors over the surface crust (Supplemental

91   Fig. S1). Oxygen profiles were recorded at 20-cm intervals from 20 to 180 cm along the 200-cm diameter of

92   the storage tank. During measurement, the microsensor was introduced stepwise into the crust at 0.5 mm

93   increments to a maximum depth of 30 mm using a motorized micromanipulator (Unisense). At each depth,

94   the microsensor was stationary for 3 s to allow gas equilibration, and then the O_2 concentration was

95   determined as the average of a 3 s reading. The signal was amplified by a multimeter (Unisense), and

96   registered by the SensorTrace PRO v3.0 software (Unisense). Nitrous oxide profiles were determined at the

97   same locations as O_2 profiles, but with a +2 mm offset to avoid any disturbance to the crust caused by the O_2

98   microsensor. The N_2O profiles were recorded with the same procedure as O_2 profiles, and initially over the

99   same depth. However, due to incidences of significant N_2O accumulation at 30 mm depth, the maximum

100   depth was extended to 60 mm starting from the 5th profile (at 100 cm distance from the edge).

101   Due to the uneven surface of the crust, a fixed depth cannot accurately define the crust-air interface. For O_2,

102   an abrupt decrease from atmospheric concentration defined the crust-air interface. For N_2O, which was

103   produced inside the crust and diffused towards the atmosphere, the crust-air interface was defined as the

104   depth where N_2O concentration dropped below the detection limit. Using these two criteria, the O_2 and N_2O

105   concentration profiles were aligned.

Methane Oxidation in Response to O_2 and N Amendments

107   Surface crust was collected from a full-scale storage tank at the biogas plant of Aarhus University in March,

108   2012. The 10-cm surface crust had developed on slurry co-digested with maize silage. Homogenized crust

109   samples were stored in closed plastic containers at 2°C until used for experiments within four weeks. Duan

110   et al. (2013) showed that MOB can survive and recover activity under these storage conditions for at least

111   three months.

112   Methane oxidation rates were determined by incubating 3-g crust samples in liquid media under a controlled

113   atmosphere. To reduce background N, crusts were washed three times by vortexing with 20 mL deionized

114   water followed by centrifugation at $10,000 \times g$ for 10 min. The washing did not remove all NH_4^+, but the

115   residual NH_4^+ was negligible compared to the received NH_4^+ amendment (Duan et al., 2013). Washed crust

116   materials were transferred to 125 mL serum bottles, and resuspended in 20 mL basal salt (BS) medium

117   prepared according to Whittenbury et al. (1970), but excluding N salts. The BS medium was dispensed using

118   a customized system designed to remove dissolved O_2 and maintain anoxia during sample preparation

119   (Supplemental Fig. S2).

120   Various treatments with combinations of different CH_4, O_2, and inorganic N were prepared (Table 2). For N

121   amendments, pre-made solutions of $(NH_4)_2SO_4$, KNO_3, or KNO_2 were injected into the serum bottles to

122 achieve the desired N concentrations. The bottles were purged using a vacuum pump and refilled with

123 helium, and this step was repeated three times to exhaust residual O_2. Then, air and ^{13}C-labeled CH_4 (99

124 atom% [13]C, ISOTEC, Miamisburg, OH, USA) were injected to achieve the desired headspace gas

125 concentrations. To meet the requirement for CO_2 by some MOB, 4 mL pure CO_2 was also added (Acha et al.,

126 2002). After gas injection, the bottles were mounted on a rotary shaker at 150 rpm for 30 min to allow for

127 liquid-gas equilibration. Headspace O_2 concentrations were verified using an Agilent 3000A MicroGC

128 (Hørsholm, Denmark) as described by (Petersen et al., 2009). For treatments with 0% O_2, residual headspace

129 O_2 concentration was undetectable (< 10–20 ppmv). The bottles were then incubated on a rotary shaker at

130 200 rpm at ca. 21°C; Duan et al. (2013) had shown that there is no gas diffusion limitation under these

131 incubation conditions. Headspace CH_4 concentrations were measured after 0, 2, 4, 6, 8, 24, 48, and 72 h

132 using a Shimadzu 14B GC as described by Duan et al. (2013).

133 In each batch of assays, a control with crust material in N-free BS medium at atmospheric O_2 concentration

134 was included to check for batch-to-batch variations in crust MOB activity, and a blank control without crust

135 material to correct for loss of pressure during repeated gas samplings.

136 First-order rate constants for the first 8 h of incubation and relative activities were calculated according to

137 Duan et al. (2013). First-order rate constants were compared between treatments using R v3.2.2 (R Core

138 Team, 2015). For each CH_4 concentration, effects of O_2 and inorganic N, and their interaction, were analyzed

139 by a two-way ANOVA. Differences between treatments were determined by Duncan's post-hoc multiple

140 comparison test.

PLFA Extraction and GC-c-IRMS Analysis

142 After incubation with ^{13}C-labeled CH_4, selected crust samples were processed for PLFA analysis (Table 2).

143 Prior to lipid extraction it was necessary to reduce the organic load since otherwise the humic material

144 would bind the chloroform phase and prevent isolation of lipid-soluble compounds. Crust samples were

145 vortexed and centrifuged for 10 min at 3000 × g to extract microbial cells. The supernatant was filtered

146   through 0.2 µm chloroform-soluble polycarbonate filters, and the material retained on the filter was used

147   for lipid extraction. Hence, lipid results refer to the fraction of extractable low particle size material only.

148   Polar lipid fatty acid methyl esters (FAMEs) from each filter were prepared as previously described by

149   Petersen et al. (2002).

150   FAMEs were analyzed using a HP6890 GC (Agilent, Santa Clara, CA, USA) coupled via a GC combustion

151   interface (Thermo Scientific, Bremen, Germany) in continuous flow mode to a Finnigan Delta^{PLUS} isotope

152   ratio mass spectrometer (Thermo Scientific, Bremen, Germany). The oxidation reactor on the interface was

153   maintained at 940 °C, the reduction reactor at 650 °C. Samples (1 µL) were injected at 240 °C in splitless

154   mode. The column temperature was held at 50 °C for 2 min, then increased at 15 °C min^{-1} to 100 °C,

155   subsequently at 2 °C min^{-1} to 220 °C, and finally at 15 °C min^{-1} to 240 °C, where the final temperature was

156   held for 5 min. Separated compounds were measured against a CO_2 reference gas calibrated with reference

157   to Vienna PeeDee belemnite. PLFAs were identified by relative retention time comparing samples against a

158   FAME standard mix (Supelco 37 component FAME mix, 47885-U, Sigma Aldrich). All $\delta^{13}C$ values were

159   corrected for the methanol C added during methanolysis:

160
$$\delta^{13}C_{FAME} = \frac{(N_{FA} + 1)\delta^{13}C_{FAME} - \delta^{13}C_{MeOH}}{N_{FA}}$$

161   where N_{FA} refers to the number of carbon atoms of the fatty acid component, $\delta^{13}C_{FAME}$ is the observed $\delta^{13}C$

162   value of the FAME, and $\delta^{13}C_{MeOH}$ is the $\delta^{13}C$ value of the methanol used for methanolysis (–37.7 ‰ ± 3.2 ‰).

163   The $\delta^{13}C$ isotope ratios were converted to atom%, and atom% excess was then calculated by subtraction of

164   an unlabeled control. The incorporation of $^{13}CH_4$ into membrane PLFAs (n_{13C}, nmol) was calculated as n_{13C} =

165   (PA$_{FAME}$ / PA$_{ISME}$) × n_{ISME} × (atom% ^{13}C excess), where PA$_{FAME}$ and PA$_{ISME}$ are peak areas of the FAME and

166   internal standard Me19:0, respectively, and n_{ISME} (nmol C) is the concentration of the internal standard fatty

167   acid. The lower limit of identified peaks corresponded to 0.1 ng ^{13}C g^{-1} crust material.

168   In view of the uncertain recovery of microbial cells following centrifugation and filtration, statistical testing

169   of treatment effects was not performed, and results will only be presented as means ± standard errors.

Results

Oxygen and N$_2$O Distribution in Natural Surface Crusts

172   Surface crusts from the two storage tanks showed a high spatial variability in shape and penetration depth of

173   individual O$_2$ and N$_2$O profiles, yet the distribution patterns were qualitatively similar between the two

174   tanks. Thus, results presented here are from one of the storage tanks only (Fig. 1).

175   Oxygen penetration depth varied from 2 to 14 mm, with either a steep or more gradual decline in

176   concentration. Irregularities such as a secondary increase following the initial decline were also observed

177   (e.g., at 60 cm).

178   Nitrous oxide profiles showed peak concentrations at 5–25 mm depth below the crust-air interface. Some

179   N$_2$O profiles consisted of more than one zone of N$_2$O accumulation (e.g., at 60, 100, and 160 cm). Maximum

180   N$_2$O accumulation often coincided with sub-oxic or anoxic zones indicated by O$_2$ profiles. In a few cases (e.g.,

181   at 60 and 180 cm), N$_2$O production took place where O$_2$ availability was relatively high.

Response of CH$_4$ Oxidation to O$_2$ Concentrations

183   Figure 2 shows the changes in headspace CH$_4$ concentrations during the 72-h incubation study with different

184   initial O$_2$ levels and two initial CH$_4$ levels. For both 10^2 and 10^4 ppmv CH$_4$, consistent methane consumption

185   throughout the incubation was observed only at 20% initial O$_2$, with a > 90% decline in headspace CH$_4$

186   concentrations after 72 h. In treatments with ≤ 5% initial O$_2$, CH$_4$ consumption was generally observed within

187   the first 24 h, followed by net CH$_4$ accumulation. At 0% initial O$_2$, net CH$_4$ production was observed

188   throughout the incubation.

189 The strength of methane oxidation activity was expressed as first-order rate constants during the first 8 h of

190 incubation (Fig. 3). At 10^2 ppmv initial CH_4 there were no significant differences in first-order rate constants

191 at O_2 levels from 20% down to 2%, but at 1% O_2 the rate was significantly impaired. At 10^4 ppmv initial CH_4,

192 methane oxidation rates were significantly reduced at lower O_2 levels, though not significantly different

193 between 2% and 1% O_2.

Response of CH_4 Oxidation to Interactions between O_2 and Inorganic N

195 When samples with manipulated O_2 and CH_4 concentrations were amended with inorganic N, complex

196 patterns in microbial methane oxidation were observed. For each of the two initial CH_4 concentrations, two-

197 way ANOVA showed significant effects of O_2 concentrations and N amendments, as well as their interaction,

198 on methane oxidation rates.

199 At 10^2 ppmv CH_4, first-order rate constants in all N-amended samples were lower than in the N-free control

200 (Table 3). The inhibition was strengthened at increasing concentrations of both NH_4^+ and NO_3^-. Samples

201 treated with NO_3^- consistently showed less inhibition than treatments receiving other N salts, whereas NO_2^-

202 was a potent inhibitor as indicated by similar inhibitions with 1 mM NO_2^- and 50 mM NH_4^+. At 3% O_2,

203 inhibition by individual N species and concentrations was slightly stronger than at 20% O_2, but the difference

204 was not always statistically significant.

205 At 10^4 ppmv CH_4 the order of inhibition by different N species was similar to that at 10^2 ppmv CH_4, with NO_2^-

206 as the strongest inhibitor (Table 3). Yet, several NO_3^- treatments caused a weak stimulation rather than

207 inhibition as compared to the N-free control. Generally, the N amendments inhibited methane oxidation at

208 20% O_2, but not at 3% O_2, where low rates were already observed in the N-free control. One exception,

209 though, was the inhibition caused by the treatment with 50 mM NH_4^+.

13C Incorporation into C16 and C18 PLFAs

The yields of PLFA varied considerably between samples, and ^{13}C incorporation was below the detection limit for several PLFAs, precluding a detailed quantitative analysis. Instead of absolute PLFA concentrations, an index based on peak area was calculated (Fig. 4, a1–a4). Recovery of ^{13}C PLFAs was consistently low in incubations with 10^2 ppmv CH_4 (Fig. 4, a1). At 10^4 ppmv CH_4 there was an 8–9 times higher ^{13}C recovery in PLFAs at 20% and 3% O_2 than at 1% O_2 (Fig. 4, a2). While NH_4^+ and NO_3^- considerably reduced ^{13}C recovery, NO_2^- caused no or only moderate inhibition of ^{13}C recovery (Fig. 4, a3 and a4). The total recovery of ^{13}C was 5–15 times higher with NO_2^- amendment than with the other two N species.

Two ^{13}C-labeled PLFA clusters, C_{16} and C_{18}, were defined in accordance with the predominance of these PLFAs in Type I and Type II MOB, respectively (Bodelier et al., 2009). The C_{16} cluster included peaks identified as 16:0, 16:1ω6, 16:1ω7, and 16:1ω8, whereas the C_{18} cluster included 18:0, 18:1ω7, 18:1ω9, and probably also small peaks of 18:1ω8. Also, 16:1ω6 probably co-eluted with 10*Me*16:0, and 16:1ω8 with i17:0, but this did not influence the calculated ^{13}C incorporation for the cluster.

Due to the low recovery of total ^{13}C PLFA (Fig. 4, a1) and low percentage (3–9%) of ^{13}C in C_{16} and C_{18} clusters at 10^2 ppmv CH_4 (Fig. 4, b1), no detailed interpretation of these results was possible. At 10^4 ppmv CH_4 the recovery of ^{13}C in the C_{16} and C_{18} clusters together accounted for an average of 52% of ^{13}C recovered in PLFAs. A higher percentage of ^{13}C was always recovered in the C_{16} than in the C_{18} cluster, and the percentage of the C_{16} cluster was particularly high in treatments with NO_2^- amendment (Fig. 4, b3 and b4).

Discussion

Due to the heterogenous nature of surface crusts, microbial activities within this environment are controlled by physical and chemical properties of individual microsites rather than overall bulk properties. However, detailed analysis of surface crusts is challenged by the often loose and fibrous structure of the material, and this was also the case with the straw-containing cattle slurry crust used in this study. Therefore, we chose to

233   characterize O_2 and inorganic N distributions *in situ* by microsensors, while regulation of microbial activities

234   were investigated by controlled laboratory incubations. For logistic reasons, the *in situ* gas measurements

235   and laboratory incubations were performed using different surface crusts. However, previous studies have

236   shown that crusts of different origin are qualitatively similar with respect to, e.g., depth of O_2 penetration

237   and the presence of MOB (Duan et al., 2014; Hansen et al., 2009; Nielsen et al., 2010; Nielsen et al., 2013),

238   and results from the two parts are therefore analyzed and discussed together.

Effects of O_2 Limitation and N Amendments

240   Methane oxidation kinetics are complex as the reaction involves two substrates, CH_4 and O_2 (Cai and Yan,

241   1999). We were not able to monitor O_2 concentrations during incubation, but instead calculated O_2

242   consumption by MOB based on the amounts of CH_4 consumed, the stoichiometry of methane oxidation

243   (Urmann et al., 2007), and the diffusion coefficients of CH_4 and O_2 in water (Broecker and Peng, 1974)

244   (Supplemental Table S1). These calculations suggested that there was no diffusional limitation of O_2 for

245   methane oxidation, and that the amounts of O_2 used for methane oxidation were < 10% of the available O_2

246   even at 1% initial O_2. Thus, depletion of O_2 during incubation must have been mainly due to aerobic

247   processes other than methane oxidation, i.e., any O_2 limitation for MOB activity reflected competition for O_2

248   against other aerobes. Headspace CH_4 concentrations decreased exponentially during the first 8 h, indicating

249   that the rates of CH_4 uptake depended mainly on CH_4 availability. Therefore, the reaction was approximated

250   by first-order reaction kinetics, which have also been used previously in studies of microbial methane

251   oxidation (De Visscher et al., 1999; King and Schnell, 1994; King and Schnell, 1998; Petersen and Ambus,

252   2006). The apparent first-order kinetics suggest that the rate of CH_4 uptake, and thus demand for O_2, was

253   proportional to the CH_4 concentration, which explains our observation that methane oxidation became more

254   affected by O_2 limitation at 10^4 ppmv than at 10^2 ppmv CH_4 (Fig. 3).

255   The neutral to alkaline pH of slurry (Nielsen et al., 2010; Petersen and Ambus, 2006) suggests the presence

256   of free ammonia (NH_3), which is a competitive inhibitor for methane oxidation (Carlsen et al., 1991; Gulledge

257 and Schimel, 1998). In both the present (Table 3) and a previous study (Duan et al., 2013), inhibition by

258 ammonia was less at 10^4 compared to 10^2 ppmv CH_4, suggesting that competitive inhibition is important for

259 effects of ammonia. The observations that NO_2^- was a more potent inhibitor of methane oxidation than NO_3^-

260 was also consistent with the report by Duan et al. (2013), where the concentration of NO_3^- resulting in 50%

261 inhibition was 100-fold higher than that of NO_2^-. It is likely that these N species both inhibit methane

262 oxidation *via* nitrite toxicity (Stein and Klotz, 2011).

263 We further tested interactions of N inhibition with O_2 availability by comparing relative activities. If there

264 were an interaction between O_2 and inorganic N, a given N amendment would result in different degree of

265 inhibition at 20% and 3% O_2 concentrations. At 10^2 ppmv initial CH_4, 10 mM, but not 50 mM, NH_4^+ or NO_3^-

266 amendments caused a stronger inhibition at 3% than at 20% O_2 (Table 3), confirming an interaction between

267 N inhibition and O_2 limitation at low N concentrations. At 10^4 ppmv CH_4, the fact that N amendments

268 generally inhibited methane oxidation at 20% O_2 but not further at 3% O_2 suggested that high-concentration

269 methane oxidation is more sensitive to O_2 limitation rather than to N inhibition.

270 Generally, as an essential substrate for aerobic methane oxidation, O_2 has a direct and immediate effect on

271 aerobic methanotrophic activity. On the other hand, the mechanism of N inhibition on methane oxidation is

272 much more complex and may include immediate toxicity to cell growth and enzyme synthesis, as well as

273 delayed influence on microbial community composition (Bodelier and Laanbroek, 2004). The mechanisms

274 behind interactions between controlling factors in surface crusts could not be explained with the data

275 presented here, and more research is needed to further elucidate this matter.

276 ### ^{13}C PLFA Signatures for MOB

277 Type I and Type II MOB produce unique membrane PLFAs, 16:1ω8 and 18:1ω8, respectively (Bodelier et al.,

278 2009; Hanson and Hanson, 1996). These signature PLFAs are not always present, or present only in low

279 amounts. However, there is also a general predominance of C_{16} and C_{18} PLFAs among Type I and Type II

280 MOB, respectively (Bodelier et al., 2009), and this has been used to evaluate sources of methane oxidation

281   by stable isotope probing (Qiu et al., 2008). In the present study, both types of MOB were active, with Type I

282   MOB dominating the methanotrophic activity especially where CH_4 availability was high (Fig. 4, b1 and b2).

283   Molecular analyses of microflora in other crust materials likewise suggested that Type I MOB dominated the

284   methanotrophic community in terms of both diversity and abundance (Duan et al., 2014).

285   Interestingly, the incorporation of ^{13}C into PLFAs was high in surface crusts incubated with NO_2^- as compared

286   to those with other N species (Fig. 4, a3 and a4), especially considering that crusts incubated with NO_3^- had

287   over two-fold higher $^{13}CH_4$ uptake than NO_2^- treatments (data not shown). Roslev et al. (1997) reported that

288   NH_4^+ decreased C conversion efficiency and increased respiration of C assimilated by MOB, which is

289   consistent with the low ^{13}C recovery from NH_4^+ treatments in this study. However, the mechanism by which

290   NO_3^- and NO_2^- could interfere with C assimilation for MOB remains unclear. Alternative pathways for CH_4

291   uptake may have contributed to the particularly high ^{13}C assimilation in NO_2^- amended crusts. The

292   microorganism *Candidatus Methylomirabilis oxyfera* is able to couple anaerobic methane oxidation with

293   nitrite reduction (Ettwig et al., 2010), and may be widespread in natural environments (Ettwig et al., 2009;

294   Wang et al., 2012; Zhu et al., 2012). We recovered 10*Me*$C_{16:0}$ in the present study, which is characteristic of

295   the lipid profile of *M. oxyfera* (Kool et al., 2012). Still, more concrete evidence, such as the recovery of

296   specific gene markers of *M. oxyfera* (Luesken et al., 2011), is needed to confirm the presence of *M. oxyfera*

297   in surface crusts. More recently, gammaproteobacterial (Type I) methanotrophs *Methylomonas denitrificans*

298   and *Methylomicrobium album* have been reported to be able to oxidize methane under hypoxia using

299   oxidized nitrogen as electron acceptor (Kits et al., 2015a; Kits et al., 2015b). The involvement of such a

300   process would be consistent with the high proportion of C_{16} PLFAs recovered from NO_3^- and NO_2^-

301   treatments, and the genera *Methylomonas* and *Methylomicrobium* are widespread (Knief, 2015) and were

302   indeed present in surface crusts (Duan et al., 2014). However, there was no direct evidence in the present

303   study to evaluate the presence of these specific strains.

In-situ O_2 and N_2O Distribution and Implications for CH_4 Oxidation

Oxygen distribution in surface crusts vary over short distances, as shown in this and other studies (Hansen et al., 2009; Nielsen et al., 2010). Despite this variation, the depth of O_2 penetration is generally shallow and was never more than 25% of the thickness of the crust (Nielsen et al., 2010). The restriction of significant O_2 penetration is likely due to surface crusts being a floating organic structure on top of liquid slurry, where the bottom of the crust is always saturated, while aerobic processes actively consume O_2 in upper layers. Nielsen et al. (2010) proposed that trapping of gases formed in the slurry could elevate the crust above the liquid slurry phase and, as a result, improve O_2 penetration. Measurements of O_2 at a fixed depth over 48 h did indicate gas pockets that lifted the crust, but they were intermittently deflated (Supplemental Fig. S3). Structural voids in the crusts, such as pores and crevices, could also provide access for O_2 to deeper parts of the crusts, and weather conditions such as precipitation and drought will influence O_2 permeability by altering the wetness of the crust (Hansen et al., 2009).

The present study observed N_2O levels as high as 100 µmol L^{-1}, which was far above the N_2O concentrations commonly found in other environments. For example, Baral et al. (2014) and Zhou et al. (2016) reported N_2O concentrations of < 5 µmol L^{-1} near the soil surface. Careful examination of potential interferences to the microsensor is therefore warranted. Surface crusts may contain up to 300 µmol L^{-1} of H_2S (Nielsen et al., 2010), and H_2S is known to affect the signal of N_2O microsensors. However, the microsensor used here is equipped with an alkaline oxygen guard which converts incoming H_2S to ionic forms, and this offers some protection to the cathode from H_2S (Andersen et al., 2001). With the same type of microsensor used in this study, Andersen et al. (2001) found a reduction in the sensitivity towards N_2O with increasing concentrations of H_2S up to 350 µmol L^{-1}, indicating that any H_2S interference would result in lower, not higher, N_2O readings. Therefore, the high N_2O concentrations observed were not likely to be a result of H_2S interference. In the above mentioned studies where soil N_2O concentrations were <5 µmol L^{-1}, the corresponding N_2O emissions were 3.6 and 25 µmol m^{-2} h^{-1} (Baral et al., 2014; Zhou et al., 2016). For livestock slurry with surface crusts, N_2O emissions as high as 393–1,429 µmol m^{-2} h^{-1} have been reported (Hansen et al., 2009;

329   Sommer et al., 2000). Considering the relationship between N_2O concentration and emission, N_2O

330   concentrations up to 100 µmol L^{-1} in surface crusts seem plausible.

331   Maximum N_2O accumulation occurred near the oxic-anoxic interface in most cases, and therefore both

332   nitrification and denitrification were potential sources of N_2O (Braker and Conrad, 2011). Law et al. (2012)

333   found a correlation between N_2O production and ammonia oxidation rate, possibly as a result of nitrifier

334   denitrification to conserve O_2 or prevent NO_2^- toxicity (Lawton et al., 2013), and similar mechanisms could

335   lead to N_2O accumulation via ammonia oxidation in surface crusts. At or below oxic-anoxic interfaces,

336   incomplete heterotrophic denitrification was likely the main source of N_2O due to intolerance of N_2O

337   reductase towards trace O_2 (Thomson et al., 2012). Nitrous oxide could also be released as a terminal

338   product from methane oxidation coupled with partial denitrification by *M. denitrificans* (Kits et al., 2015b)

339   and *M. album* (Kits et al., 2015a; Nyerges et al., 2010), which can be enabled by hypoxia developed at the

340   oxic-anoxic interfaces. Denitrification could also act as a sink for NO_3^- or, particularly, NO_2^- which is a strong

341   inhibitor of aerobic methane oxidation. The ubiquitous presence of N_2O in the surface crusts indicated active

342   transformations of N species which could interfere with methane oxidation. Yet, as seen from the incubation

343   experiments, the effect of N species on MOB may be either inhibitory or stimulatory depending on other

344   factors. Moreover, Type I MOB utilizing NO_2^- and/or NO_3^- for methane oxidation are presumably more

345   resilient to N inhibition than others (Zhu et al., 2016). In support of this, *M. denitrificans* and *M. album* have

346   been shown to tolerate and grow under 10 mM NO_3^- (Kits et al., 2015b) and 2.5 mM NO_2^- (Nyerges et al.,

347   2010), respectively. Also, Hu and Lu (2015) found that, while NH_4^+ and NO_3^- both stimulated Type I MOB as

348   determined from *pmo*A gene copy numbers, Type II MOB were inhibited by NH_4^+ as concentrations

349   increased.

350   Clearly, various physio-chemical and biological properties are involved in regulating methane oxidation in

351   surface crust. Firstly, the heterogeneous structure of the crust adds complexity to the distribution of gases.

352   Secondly, there are complex interactions between CH_4 and O_2 levels, and inorganic N species and

353   concentration, with respect to methanotrophic activity. In parts of the crust where CH_4 availability is

relatively low, moderate O_2 limitation probably has little impact on aerobic methane oxidation activity, whereas N inhibition could be significant depending on N species and concentration. In contrast, in parts of the crust with high CH_4 availability, O_2 limitation is likely the main control of aerobic methane oxidation, and inhibition due to inorganic N is only important where O_2 is not limiting.

Conclusions

Microsensor measurements of *in situ* O_2 and N_2O profiles revealed shallow penetration of O_2 into slurry surface crusts and active N transformations around oxic-anoxic interfaces. Laboratory incubations suggested that O_2 availability was more important to high-concentration than low-concentration methane oxidation, and there were complex interactions between inorganic N and O_2 limitation. The incorporation of ^{13}C from CH_4 into membrane PLFAs indicated that both Type I and Type II MOB were actively involved in methane oxidation, but with Type I MOB dominating the activity at high CH_4 concentrations. These observations together imply that manipulation of storage conditions to increase headspace CH_4 concentration, as proposed by Petersen and Miller (2006), could stimulate methane oxidation by Type I MOB in the upper parts of the crust where O_2 is non-limiting and mineral N availability low.

Acknowledgements

References

Acha, V., J. Alba and F. Thalasso. 2002. The absolute requirement for carbon dioxide for aerobic methane oxidation by a methanotrophic-heterotrophic soil community of bacteria. Biotechnology Letters 24: 675-679. doi:10.1023/a:1015265530501.

Amaral, J.A., C. Archambault, S.R. Richards and R. Knowles. 1995. Denitrification associated with groups I and II methanotrophs in a gradient enrichment system. FEMS Microbiology Ecology 18: 289-298.

Amaral, J.A. and R. Knowles. 1995. Growth of methanotrophs in methane and oxygen counter gradients. FEMS Microbiology Letters 126: 215-220. doi:10.1111/j.1574-6968.1995.tb07421.x.

Andersen, K., T. Kjær and N.P. Revsbech. 2001. An oxygen insensitive microsensor for nitrous oxide. Sensors and Actuators B: Chemical 81: 42-48. doi:http://dx.doi.org/10.1016/S0925-4005(01)00924-8.

Baral, K.R., A.G. Thomsen, J.E. Olesen and S.O. Petersen. 2014. Controls of nitrous oxide emission after simulated cattle urine deposition. Agriculture, Ecosystems & Environment 188: 103-110. doi:http://dx.doi.org/10.1016/j.agee.2014.02.029.

Bodelier, P.L.E. 2011. Interactions between nitrogenous fertilizers and methane cycling in wetland and upland soils. Current Opinion in Environmental Sustainability 3: 379-388. doi:http://dx.doi.org/10.1016/j.cosust.2011.06.002.

Bodelier, P.L.E., M.-J. Bar Gillisen, K. Hordijk, J.S. Sinninghe Damste, W.I.C. Rijpstra, J.A.J. Geenevasen, et al. 2009. A reanalysis of phospholipid fatty acids as ecological biomarkers for methanotrophic bacteria. ISME J 3: 606-617. doi:10.1038/ismej.2009.6.

Bodelier, P.L.E. and H.J. Laanbroek. 2004. Nitrogen as a regulatory factor of methane oxidation in soils and sediments. FEMS Microbiology Ecology 47: 265-277. doi:10.1016/s0168-6496(03)00304-0.

Bollmann, A. and R. Conrad. 1998. Influence of O2 availability on NO and N2O release by nitrification and denitrification in soils. Global Change Biology 4: 387-396. doi:10.1046/j.1365-2486.1998.00161.x.

Bosse, U., P. Frenzel and R. Conrad. 1993. Inhibition of methane oxidation by ammonium in the surface layer of a littoral sediment. Fems Microbiology Ecology 13: 123-134. doi:10.1016/0168-6496(93)90030-b.

Braker, G. and R. Conrad. 2011. Chapter 2: Diversity, Structure, and Size of N$_2$O-Producing Microbial Communities in Soils – What Matters for Their Functioning? In: S. S. Allen I. Laskin and M. G. Geoffrey, editors, Advances in Applied Microbiology. Academic Press. p. 33-70.

Broecker, W.S. and T.H. Peng. 1974. Gas exchange rates between air and sea. Tellus 26: 21-35. doi:10.1111/j.2153-3490.1974.tb01948.x.

Cai, Z.C. and X.Y. Yan. 1999. Kinetic model for methane oxidation by paddy soil as affected by temperature, moisture and N addition. Soil Biology & Biochemistry 31: 715-725.

Carlsen, H.N., L. Joergensen and H. Degn. 1991. Inhibition by ammonia of methane utilization in Methylococcus capsulatus (Bath). Applied Microbiology and Biotechnology 35: 124-127. doi:10.1007/bf00180649.

Damgaard, L.R. and N.P. Revsbech. 1997. A Microscale Biosensor for Methane Containing Methanotrophic Bacteria and an Internal Oxygen Reservoir. Analytical Chemistry 69: 2262-2267. doi:10.1021/ac9611576.

De Beer, D., A. Schramm, C.M. Santegoeds and M. Kuhl. 1997. A nitrite microsensor for profiling environmental biofilms. Applied and Environmental Microbiology 63: 973-977.

De Beer, D., J.-P.R.A. Sweerts and J.C. van den Heuvel. 1991. Microelectrode measurement of ammonium profiles in freshwater sediments. FEMS Microbiology Letters 86: 1-6. doi:10.1111/j.1574-6968.1991.tb04789.x.

De Visscher, A., D. Thomas, P. Boeckx and O. Van Cleemput. 1999. Methane Oxidation in Simulated Landfill Cover Soil Environments. Environmental Science & Technology 33: 1854-1859. doi:10.1021/es9900961.

Duan, Y.-F., W. Abu Al-Soud, A. Brejnrod , S.J. Sørensen, L. Elsgaard, S.O. Petersen, et al. 2014. Methanotrophs, methanogens and microbial community structure in livestock slurry surface crusts. Journal of Applied Microbiology 117: 1066–1078. doi:10.1111/jam.12584.

Duan, Y.-F., L. Elsgaard and S.O. Petersen. 2013. Inhibition of methane oxidation in a slurry surface crust by inorganic N: An incubation study. Journal of Environmental Quality 42: 507-515. doi:10.2134/jeq2012.0230.

Dunfield, P. and R. Knowles. 1995. Kinetics of inhibition of methane oxidation by nitrate, nitrite, and ammonium in a humisol. Applied and Environmental Microbiology 61: 3129-3135.

Ettwig, K.F., T.v. Alen, K.T.v.d. Pas-Schoonen, M.S.M. Jetten and M. Strous. 2009. Enrichment and molecular detection of denitrifying methanotrophic bacteria of the NC10 phylum. Applied and Environmental Microbiology 75: 3656-3662. doi:10.1128/aem.00067-09.

Ettwig, K.F., M.K. Butler, D. Le Paslier, E. Pelletier, S. Mangenot, M.M.M. Kuypers, et al. 2010. Nitrite-driven anaerobic methane oxidation by oxygenic bacteria. Nature 464: 543-548. doi:10.1038/nature08883.

Francesco, N.T., S. Mirella, R. Simone, F. Alessandro, F. Nuala and S. Pete. 2013. The FAOSTAT database of greenhouse gas emissions from agriculture. Environmental Research Letters 8: 015009.

Graham, D.W., J.A. Chaudhary, R.S. Hanson and R.G. Arnold. 1993. Factors affecting competition between type I and type II methanotrophs in two-organism, continuous-flow reactors. Microbial Ecology 25: 1-17. doi:10.1007/bf00182126.

Gulledge, J. and J.P. Schimel. 1998. Low-Concentration Kinetics of Atmospheric CH4 Oxidation in Soil and Mechanism of NH4+ Inhibition. Applied and Environmental Microbiology 64: 4291-4298.

Hansen, R.R., D.A. Nielsen, A. Schramm, L.P. Nielsen, N.P. Revsbech and M.N. Hansen. 2009. Greenhouse Gas Microbiology in Wet and Dry Straw Crust Covering Pig Slurry. Journal of Environmental Quality 38: 1311-1319. doi:10.2134/jeq2008.0336.

Hanson, R.S. and T.E. Hanson. 1996. Methanotrophic bacteria. Microbiological Reviews 60: 439-471.

Hu, A. and Y. Lu. 2015. The differential effects of ammonium and nitrate on methanotrophs in rice field soil. Soil Biology and Biochemistry 85: 31-38. doi:http://dx.doi.org/10.1016/j.soilbio.2015.02.033.

King, G.M. and S. Schnell. 1994. Ammonium and Nitrite Inhibition of Methane Oxidation by Methylobacter albus BG8 and Methylosinus trichosporium OB3b at Low Methane Concentrations. Applied and Environmental Microbiology 60: 3508-3513.

King, G.M. and S. Schnell. 1998. Effects of Ammonium and Non-Ammonium Salt Additions on Methane Oxidation by Methylosinus trichosporium OB3b and Maine Forest Soils. Applied and Environmental Microbiology 64: 253-257.

Kits, K.D., D.J. Campbell, A.R. Rosana and L.Y. Stein. 2015a. Diverse electron sources support denitrification under hypoxia in the obligate methanotroph Methylomicrobium album strain BG8. Frontiers in Microbiology 6: 1072. doi:10.3389/fmicb.2015.01072.

Kits, K.D., M.G. Klotz and L.Y. Stein. 2015b. Methane oxidation coupled to nitrate reduction under hypoxia by the Gammaproteobacterium Methylomonas denitrificans, sp. nov. type strain FJG1. Environmental Microbiology 17: 3219-3232. doi:10.1111/1462-2920.12772.

Knief, C. 2015. Diversity and Habitat Preferences of Cultivated and Uncultivated Aerobic Methanotrophic Bacteria Evaluated Based on pmoA as Molecular Marker. Frontiers in Microbiology 6. doi:10.3389/fmicb.2015.01346.

Kool, D.M., B. Zhu, W.I.C. Rijpstra, M.S.M. Jetten, K.F. Ettwig and J.S. Sinninghe Damsté. 2012. Rare Branched Fatty Acids Characterize the Lipid Composition of the Intra-Aerobic Methane Oxidizer "Candidatus Methylomirabilis oxyfera". Applied and Environmental Microbiology 78: 8650-8656. doi:10.1128/aem.02099-12.

Larsen, L.H., N.P. Revsbech and S.J. Binnerup. 1996. A microsensor for nitrate based on immobilized denitrifying bacteria. Applied and Environmental Microbiology 62: 1248-1251.

Law, Y., B.-J. Ni, P. Lant and Z. Yuan. 2012. N2O production rate of an enriched ammonia-oxidising bacteria culture exponentially correlates to its ammonia oxidation rate. Water Research 46: 3409-3419. doi:10.1016/j.watres.2012.03.043.

Lawton, T.J., K.E. Bowen, L.A. Sayavedra-Soto, D.J. Arp and A.C. Rosenzweig. 2013. Characterization of a Nitrite Reductase Involved in Nitrifier Denitrification. Journal of Biological Chemistry 288: 25575-25583. doi:10.1074/jbc.M113.484543.

Liu, L. and T.L. Greaver. 2009. A review of nitrogen enrichment effects on three biogenic GHGs: the CO2 sink may be largely offset by stimulated N2O and CH4 emission. Ecology Letters 12: 1103-1117. doi:10.1111/j.1461-0248.2009.01351.x.

Luesken, F.A., B. Zhu, T.A. van Alen, M.K. Butler, M. Rodriguez Diaz, B. Song, et al. 2011. pmoA primers for detection of anaerobic methanotrophs. Applied and Environmental Microbiology. doi:10.1128/aem.02960-10.

Melse, R.W. and A.W. van der Werf. 2005. Biofiltration for Mitigation of Methane Emission from Animal Husbandry. Environmental Science & Technology 39: 5460-5468. doi:10.1021/es048048q.

Nielsen, D.A., L.P. Nielsen, A. Schramm and N.P. Revsbech. 2010. Oxygen Distribution and Potential Ammonia Oxidation in Floating, Liquid Manure Crusts. J. Environ. Qual. 39: 1813-1820. doi:10.2134/jeq2009.0382.

Nielsen, D.A., A. Schramm, L.P. Nielsen and N.P. Revsbech. 2013. Seasonal Methane Oxidation Potential in Manure Crusts. Applied and Environmental Microbiology 79: 407-410. doi:10.1128/aem.02278-12.

Nyerges, G., S.-K. Han and L.Y. Stein. 2010. Effects of Ammonium and Nitrite on Growth and Competitive Fitness of Cultivated Methanotrophic Bacteria. Applied and Environmental Microbiology 76: 5648-5651. doi:10.1128/aem.00747-10.

Petersen, S. and P. Ambus. 2006. Methane Oxidation in Pig and Cattle Slurry Storages, and Effects of Surface Crust Moisture and Methane Availability. Nutrient Cycling in Agroecosystems 74: 1-11. doi:10.1007/s10705-005-3822-6.

Petersen, S.O., B. Amon and A. Gattinger. 2005. Methane Oxidation in Slurry Storage Surface Crusts. J. Environ. Qual. 34: 455-461. doi:10.2134/jeq2005.0455.

Petersen, S.O., P.S. Frohne and A.C. Kennedy. 2002. Dynamics of a Soil Microbial Community under Spring Wheat. Soil Science Society of America Journal 66: 826-833. doi:10.2136/sssaj2002.8260.

Petersen, S.O. and D.N. Miller. 2006. Greenhouse gas mitigation by covers on livestock slurry tanks and lagoons? Journal of the Science of Food and Agriculture 86: 1407-1411. doi:10.1002/jsfa.2543.

Petersen, S.O., M. Skov, P. Drøscher and A.P.S. Adamsen. 2009. Pilot Scale Facility To Determine Gaseous Emissions From Livestock Slurry During Storage. J. Environ. Qual. 38: 1560-1568. doi:10.2134/jeq2008.0376.

Qiu, Q., M. Noll, W.-R. Abraham, Y. Lu and R. Conrad. 2008. Applying stable isotope probing of phospholipid fatty acids and rRNA in a Chinese rice field to study activity and composition of the methanotrophic bacterial communities in situ. ISME J 2: 602-614.

Revsbech, N.P. 2005. Analysis of Microbial Communities with Electrochemical Microsensors and Microscale Biosensors. In: R. L. Jared, editor Methods in Enzymology. Academic Press. p. 147-166.

Roslev, P., N. Iversen and K. Henriksen. 1997. Oxidation and assimilation of atmospheric methane by soil methane oxidizers. Applied and Environmental Microbiology 63: 874-880.

Sommer, S., S. Petersen, P. Sørensen, H. Poulsen and H. Møller. 2007. Methane and carbon dioxide emissions and nitrogen turnover during liquid manure storage. Nutrient Cycling in Agroecosystems 78: 27-36. doi:10.1007/s10705-006-9072-4.

Sommer, S.G., S.O. Petersen and H.T. Søgaard. 2000. Greenhouse Gas Emission from Stored Livestock Slurry. Journal of Environmental Quality 29: 744-751. doi:10.2134/jeq2000.00472425002900030009x.

Stein, L.Y. and M.G. Klotz. 2011. Nitrifying and denitrifying pathways of methanotrophic bacteria. Biochemical Society Transactions 39: 1826-1831. doi:10.1042/bst20110712.

Thomson, A.J., G. Giannopoulos, J. Pretty, E.M. Baggs and D.J. Richardson. 2012. Biological sources and sinks of nitrous oxide and strategies to mitigate emissions. Philosophical Transactions of The Royal Society B 367: 1157-1168. doi:10.1098/rstb.2011.0415.

Urmann, K., E.S. Norina, M.H. Schroth and J. Zeyer. 2007. Methanotrophic activity in a diffusive methane/oxygen counter-gradient in an unsaturated porous medium. Journal of Contaminant Hydrology 94: 126-138. doi:10.1016/j.jconhyd.2007.05.006.

Wang, Y., G. Zhu, H.R. Harhangi, B. Zhu, M.S.M. Jetten, C. Yin, et al. 2012. Co-occurrence and distribution of nitrite-dependent anaerobic ammonium and methane-oxidizing bacteria in a paddy soil. FEMS Microbiology Letters 336: 79-88. doi:10.1111/j.1574-6968.2012.02654.x.

Wang, Z.-P. and P. Ineson. 2003. Methane oxidation in a temperate coniferous forest soil: effects of inorganic N. Soil Biology and Biochemistry 35: 427-433. doi:10.1016/s0038-0717(02)00294-8.

Welte, C.U., O. Rasigraf, A. Vaksmaa, W. Versantvoort, A. Arshad, H.J.M. Op den Camp, et al. 2016. Nitrate- and nitrite-dependent anaerobic oxidation of methane. Environmental Microbiology Reports 8: 941-955. doi:10.1111/1758-2229.12487.

Whittenbury, R., K.C. Phillips and J.F. Wilkinson. 1970. Enrichment, Isolation and Some Properties of Methane-utilizing Bacteria. Journal of General Microbiology 61: 205-218. doi:10.1099/00221287-61-2-205.

Zhou, Z., X. Xu, Z. Bi, L. Li, B. Li and Z. Xiong. 2016. Soil concentration profiles and diffusion and emission of nitrous oxide influenced by the application of biochar in a rice-wheat annual rotation system. Environmental Science and Pollution Research 23: 7949-7961. doi:10.1007/s11356-015-5929-x.

Zhu, B., G. van Dijk, C. Fritz, A.J.P. Smolders, A. Pol, M.S.M. Jetten, et al. 2012. Anaerobic Oxidization of Methane in a Minerotrophic Peatland: Enrichment of Nitrite-Dependent Methane-Oxidizing Bacteria. Applied and Environmental Microbiology 78: 8657-8665. doi:10.1128/aem.02102-12.

Zhu, J., Q. Wang, M. Yuan, G.-Y.A. Tan, F. Sun, C. Wang, et al. 2016. Microbiology and potential applications of aerobic methane oxidation coupled to denitrification (AME-D) process: A review. Water Research 90: 203-215. doi:http://dx.doi.org/10.1016/j.watres.2015.12.020.
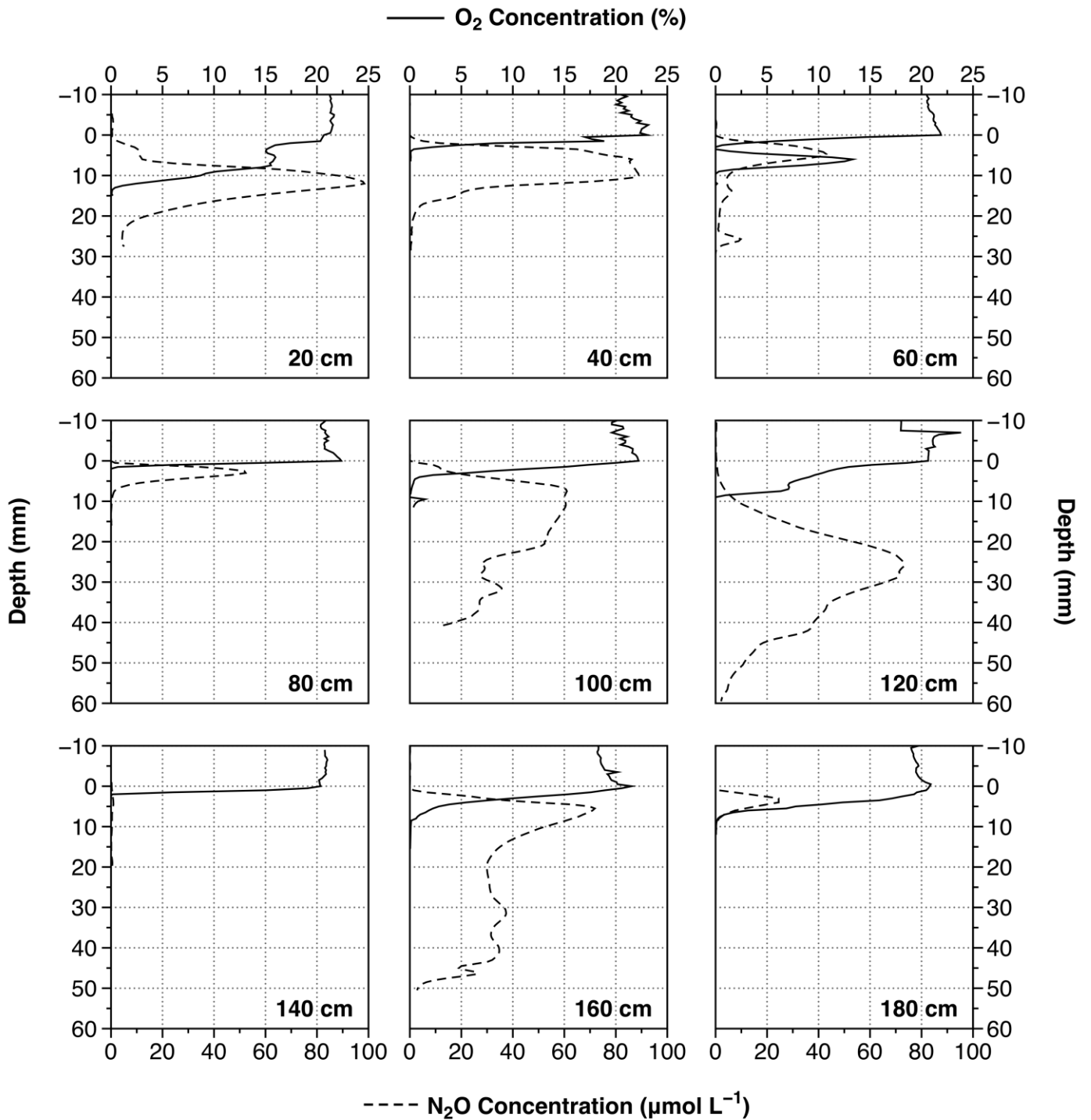
Figure 1: Profiles of oxygen (O₂, solid line, top X-axis) and nitrous oxide (N₂O, dashed line, bottom X-axis) profiles in a surface crust measured using microsensors at 20 cm intervals along the 200-cm diameter of a slurry storage tank. Distances of the sampling points from the edge of the tank are indicated on the bottom-right corner of each panel. Oxygen was traced to a depth of 30 mm in all cases; N₂O was traced to a depth of 30 mm at 20–80 cm and to a depth of 60 mm at 100–180 cm.
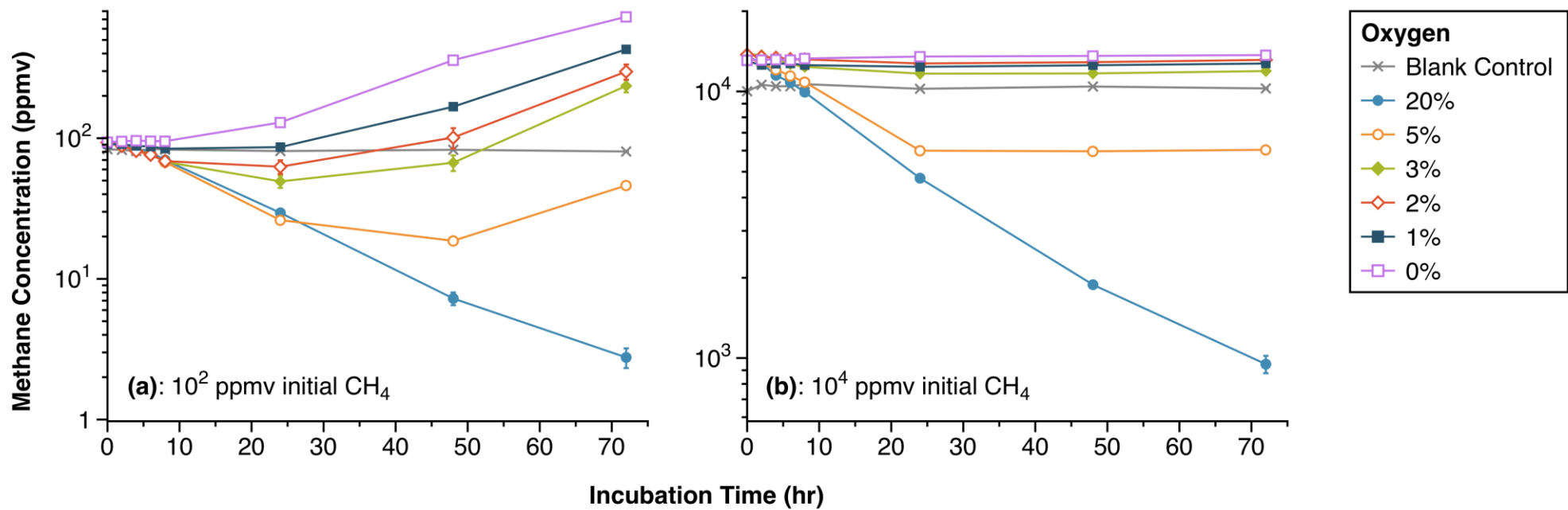
Figure 2: Dynamics of CH_4 concentrations during a 72-h incubation of slurry surface crusts with initial O_2 concentrations of 20, 5, 3, 2, 1, and 0%, and with initial CH_4 concentrations of 10^2 ppmv (a) and 10^4 ppmv (b). Blank control contained 20% initial headspace O_2 and no crust material. Each point represents the mean of triplicate assays, and error bars show standard error.
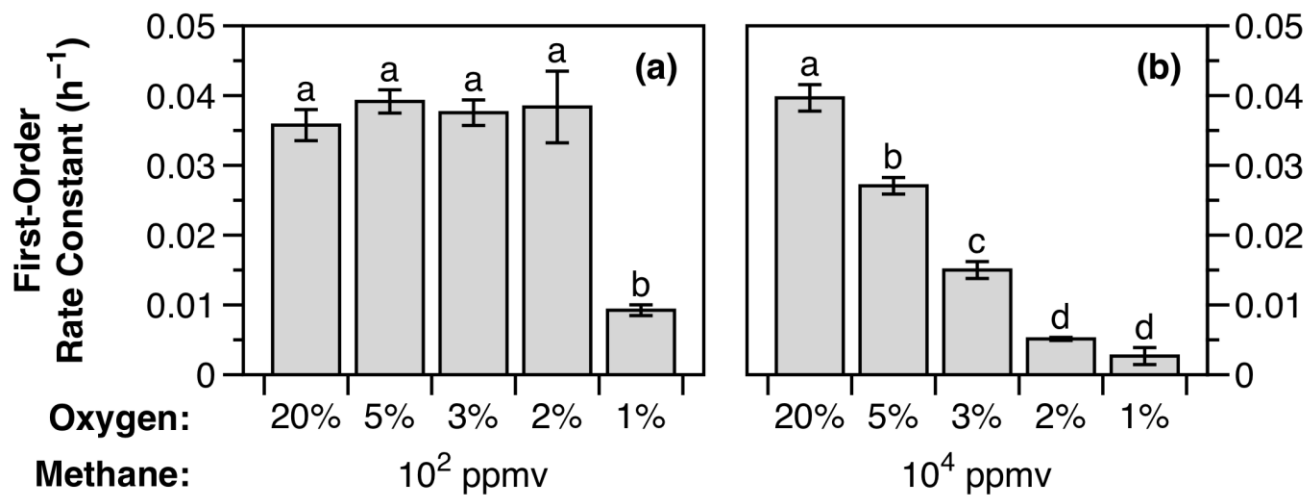
Figure 3: First-order rate constants of potential CH_4 oxidation under different O_2 and CH_4 concentrations during the first 8 h of incubation. The bars show the mean of triplicate assays, and the error bars show standard error. For each CH_4 concentration, bars denoted with the same letter on top are not significantly different at $\alpha = 0.05$.
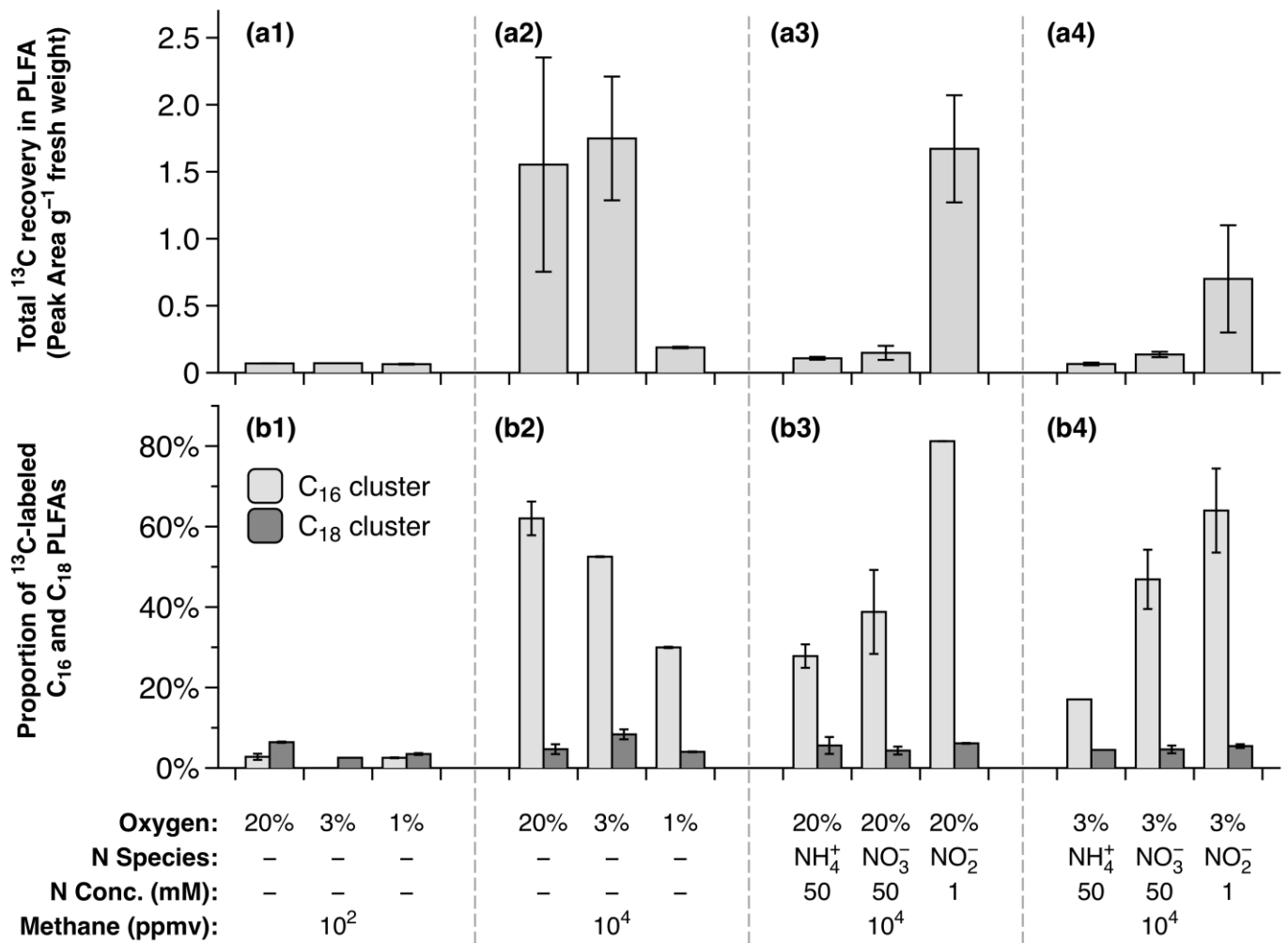
Figure 4: Total recovery of ^{13}C in PLFA (expressed as peak area per gram fresh crust) derived from incubation of surface crusts with $^{13}CH_4$ (a1–a4), and proportions of ^{13}C incorporation into PLFA belonging to C_{16} or C_{18} clusters (b1–b4) at different combinations of O_2, CH_4, and inorganic N availability. Data shown are means and standard errors of two replicates.

Table 1: Selected chemical properties of various livestock slurries and surface crusts from previous studies.

Sample	Surface Crust			Slurry	
	NH_4^+	NO_3^-	NO_2^-	pH	NH_4^+
	µmol kg^{-1} WW*	µmol kg^{-1} WW	µmol kg^{-1} WW		mM
Cattle slurry surface crusts developed for 3 years (Duan et al., 2013)	116.3	370.9	n.a.[#]	n.a.	n.a.
Various cattle and swine slurries and surface crusts (Nielsen et al., 2010)	n.a.	7– 3,602	2–98,000	6.96–7.7	84–205
Surface crusts of various dryness (Hansen et al., 2009)	n.a.	290–35,000	80–1,990	7.7	175
Various cattle and swine slurries (Sommer et al., 2007)	n.a.	n.a.	n.a.	n.a.	79–257
Surface crusts (Petersen et al., 2006)	1,432–54,923	91–16,378	3–50	7.13–8.89	1.7–69
Digested cattle slurry (Clemens et al., 2006)	n.a.	n.a.	n.a.	7.4–7.8	85–127

* WW, wet weight.
[#] n.a., value not reported.

Table 2: Combinations of CH_4, O_2, and inorganic N amendments used in this study. The values indicate the number of replicates prepared. Treatments marked with asterisks (*) were used for analysis of ^{13}C-labelled phosphate lipid fatty acids (PLFAs).

N Species and Concentrations		CH₄: O_2:	10² ppmv						10⁴ ppmv					
			0%	1%	2%	3%	5%	20%	0%	1%	2%	3%	5%	20%
None			3	3*	3	3*	3	3*	3	3*	3	3*	3	3*
NH₄⁺	10 mM					2		2				2		2
	50 mM					2		2				2*		2*
NO₃⁻	10 mM					2		2				2		2
	50 mM					2		2				2*		2*
NO₂⁻	1 mM					2		2				2*		2*

Table 3: First-order rate constants (h^{-1}) of CH_4 oxidation in slurry surface crust samples under different O_2 concentrations and N amendments. Numbers in parentheses indicate relative activity (the ratio of the treatment activity as compared to the activity of the N-free control). Under each CH_4 concentration, values followed by the same letter are not significantly different at α = 0.05.

N Species and Concentrations		First-Order Rate Constants (h^{-1})			
		10^2 ppmv CH_4		10^4 ppmv CH_4	
		20% O_2	3% O_2	20% O_2	3% O_2
None		0.036 (1.00) a	0.037 (1.00) a	0.040 (1.00) b	0.016 (1.00) e
NH_4^+	10 mM	0.015 (0.42) d	0.010 (0.27) ef	0.031 (0.78) c	0.017 (1.06) e
	50 mM	0.007 (0.19) fg	0.005 (0.14) g	0.013 (0.33) e	0.005 (0.31) f
NO_3^-	10 mM	0.029 (0.81) b	0.022 (0.59) c	0.054 (1.35) a	0.022 (1.38) d
	50 mM	0.017 (0.47) d	0.013 (0.35) de	0.028 (0.70) c	0.021 (1.31) d
NO_2^-	1 mM	0.008 (0.22) fg	0.008 (0.22) fg	0.016 (0.40) e	0.017 (1.06) e

Methanotrophic activity in slurry surface crusts as influenced by CH₄, O₂, and inorganic N

Yun-Feng Duan [1] *, Sabine Reinsch [2] #, Per Ambus [2] §, Lars Elsgaard [1], and Søren O. Petersen [1]

[1] Department of Agroecology, Aarhus University, Blichers Allé 20, DK-8830 Tjele, Denmark

[2] Department of Chemical and Biochemical Engineering, Technical University of Denmark, Frederiksborgvej 399, DK-4000 Roskilde, Denmark

* Corresponding Author: Yun-Feng Duan, Department of Agroecology, Aarhus University, Blichers Allé 20, DK-8830 Tjele, Denmark; E-mail: Kevin.YF.Duan@gmail.com.

Present address: Centre for Ecology and Hydrology, Deiniol Rd, Bangor Gwynedd, LL57 2 UW, UK

§ Present address: Department of Geosciences and Natural Resource Management, University of Copenhagen, Øster Voldgade 10, DK-1350 Copenhagen, Denmark

(a). The 200-cm long aluminum bar with distance marks.

(b). The aluminum bar installed on the inner rim of the slurry tank.

(c). The motorized micromanipulator mounted on the aluminum bar.

(d). The microsensor fixed to the micromanipulator.

Figure S1: Custom-made mounting system for *in situ* measurement of O_2 and N_2O profiles using microsensors.

A 200-cm long aluminum bar with mm-scale distance marks (a) was installed on the inner rim of the storage tank, approximately 40 cm above the surface crust (b). A computer-controlled motorized micromanipulator (Unisense, Aarhus, Denmark) capable of vertical movement was mounted on a custom-made rack, which could be moved manually along the length of the aluminum bar (c). The microsensor was fixed to the micromanipulator using a rubber-lined clamp (d). When installed at the initial position for measurement, the tip of the microsensor was approximately 1 cm above the surface of the crust. During measurements, a cover was placed loosely over the storage tank to avoid heating of the surface crust by direct insolation.

When measurement at one sampling point was completed, the microsensor was retreated to initial position and temporarily detached from the micromanipulator to protect the tip from breaking during movement, and reinstalled after the micromanipulator had been moved to the next sampling point.
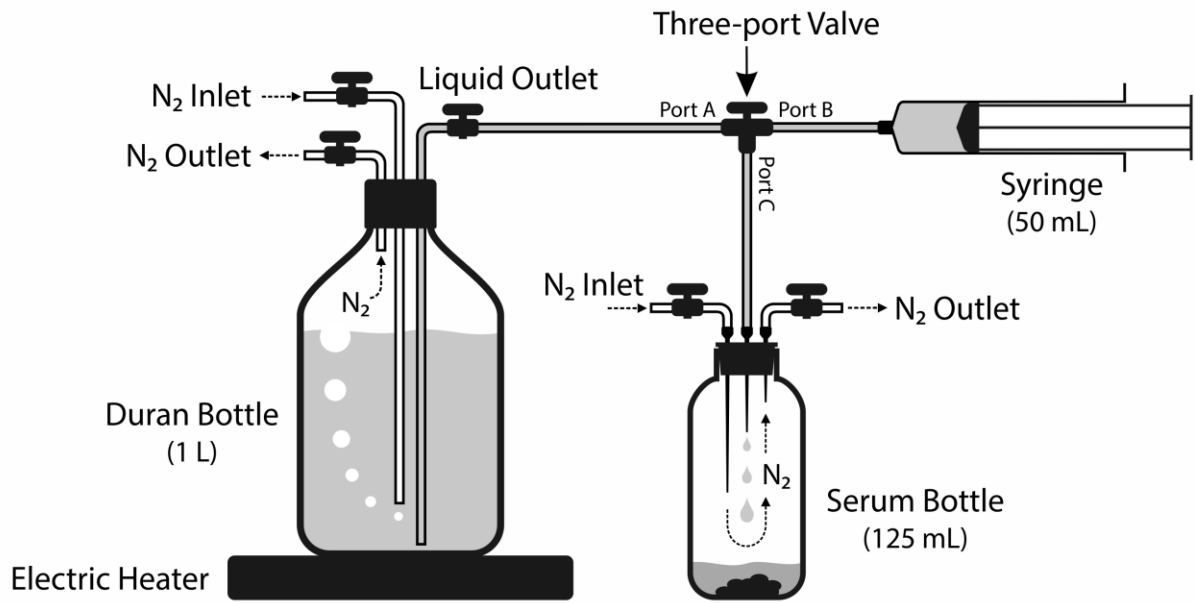
Figure S2: Diagram of the setup to prepare and distribute anoxic incubation medium.

A Duran bottle was modified to have three plastic tubes inserted through the cap: one as N_2 inlet, one as N_2 outlet, and the third as liquid outlet. The Duran bottle was filled with BS medium to ca. 70% of its volume and placed on an electric heater with the cap tightly secured. The BS medium was heated to the boiling point while bubbled with pure N_2 for at least 30 min, and then cooled to room temperature still under N_2 bubbling. Then, the N_2 outlet was closed and the liquid outlet valve was opened, and the entire tubing was flushed and filled with anoxic BS medium by the build-up of gas pressure inside the Duran bottle. When distributing BS medium to the serum bottle, a needle connected to pure N_2 flow was first inserted into the serum bottle through the rubber stopper and then, a second needle was inserted as N_2 outlet. The serum bottle was flushed with N_2 for 10 sec, and then a third needle connected to the three-port valve was inserted. Ports A and B of the three-port valve were opened while C was closed, and the syringe was filled with 20 mL incubation medium. Then, ports B and C were opened and A was closed and the incubation medium was injected from the syringe into the serum bottle while the bottle was being flushed by pure N_2.
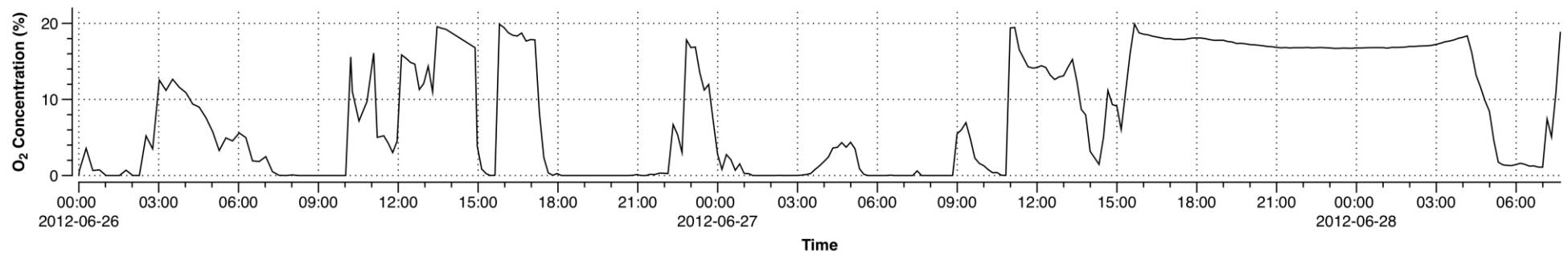
Figure S3: Dynamics of O_2 concentration at a fixed depth in a surface crust over 48 hours. The storage tank was covered to eliminate wind effect but was passively ventilated. The microsensor was initially fixed in a position where the tip just touched the surface of the crust. Oxygen concentrations were measured every 10–15 min as described in the manuscript. The peaks in O_2 profile showed that the microsensor was alternately exposed to atmospheric O_2 and more anaerobic conditions. This indicated that the surface of the crust periodically rose up and moved down, likely due to inflation and deflation of gas pockets underneath the crust.

Table S1: Oxygen Consumption during CH_4 oxidation at 10,000 ppmv initial CH_4.

Initial State (time 0)		After 8 h		
Headspace O_2 (%)	Dissolved O_2 (µM)	CH_4 Consumed (µM)	O_2 Consumed (µM)	O_2 Remaining (µM)
20	256.0	4.92	9.84	246.2
3	38.4	1.95	3.90	34.5
1	12.8	0.57	1.14	11.7

- Stoichiometry of CH_4 oxidation is:

$$CH_4 + (2-x)O_2 \longrightarrow (1-x)CO_2 + xCH_2O + (2-x)H_2O$$,
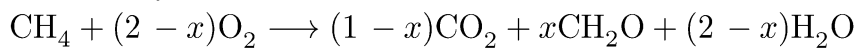
  where *x* is the fraction of carbon that is assimilated into biomass (CH_2O) (Urmann et al., 2007). Therefore, CH_4 to O_2 ratio in CH_4 oxidation theoretically ranges between 1:1 (100% C assimilation) and 1:2 (no C assimilation). In this calculation, we assumed maximum O_2 consumption, i.e. a CH_4 to O_2 ratio of 1:2.

- Henry's Law constant (*K*) for O_2 and CH_4 are 1.28 and 1.34 mmol L^{-1} atm^{-1}, respectively.

- Dissolved O_2 was calculated as: $K \times$ [Headspace O_2].

- Diffusivities of dissolved O_2 and CH_4 in water at 20°C are 2.06 and 1.75×10^{-5} cm^2 sec^{-1}, respectively (Broecker and Peng, 1974). Therefore, there's no diffusion limit of O_2 for CH_4 oxidation.